NAR Cancer, 2024, **6**, zcae042
https://doi.org/10.1093/narcan/zcae042
Advance access publication date: 30 October 2024
Cancer Gene Regulation, Chromatin, and Epigenetics

OXFORD

Sensitization of melanoma cells to standard chemotherapy: G-quadruplex binders as synergistic agents

Carolina Persico[1], Nunzia Iaccarino[1], Francesca Romano[1], Mariateresa Giustiniano[1], Camilla Russo[1], Sonia Laneri[1], Ritamaria Di Lorenzo[1], Immacolata Aiello[1], Sara Abate[1], Luana Izzo[1], Francesco Merlino[1], Diego Brancaccio[1], Bruno Pagano[1], Jussara Amato[1], Simona Marzano[1], Federica D'Aria[1], Stefano De Tito[2,*], Anna Di Porzio[1,*] and Antonio Randazzo[1,*]

[1]Department of Pharmacy, University of Naples Federico II, Via D. Montesano 49, 80131 Naples, Italy
[2]The Molecular Cell Biology of Autophagy, The Francis Crick Institute, 1 Midland Road, London NW1 1AT, UK

[*]To whom correspondence should be addressed. Tel: +39 081 678514; Email: antonio.randazzo@unina.it
Correspondence may also be addressed to Anna Di Porzio. Tel: +39 081 678111; Email: anna.diporzio@unina.it
Correspondence may also be addressed to Stefano De Tito. Tel: +44 07576579808; Email: stefano.de-tito@crick.ac.uk

Abstract

The use of chemotherapeutics has achieved considerable success in cancer therapy; however, their toxicity can severely impact patients' health. In this study, aiming to reduce the doses and potential side effects of traditional chemotherapeutics, we systematically treated A375MM human melanoma cells with seven clinically approved antineoplastic drugs, in combination with three well-characterized G-quadruplex (G4) ligands, using either simultaneous or sequential dosing schedules. Interestingly, the G4 binders synergized with most of the investigated anticancer drugs, with the degree of synergism being strictly dependent on both the treatment schedule and the drug sequence employed. Notably, some of the synergistic combinations showed selective toxicity toward melanoma cells over nontumorigenic human keratinocytes. Furthermore, immunofluorescence experiments highlighted the potential implication of G4 structures in the molecular mechanisms driving the synergistic interaction between some chemotherapeutics and G4 binders. Overall, our systematic study supports the combination of G4-interacting molecules with standard antineoplastic drugs as a promising antitumor strategy.

Graphical abstract

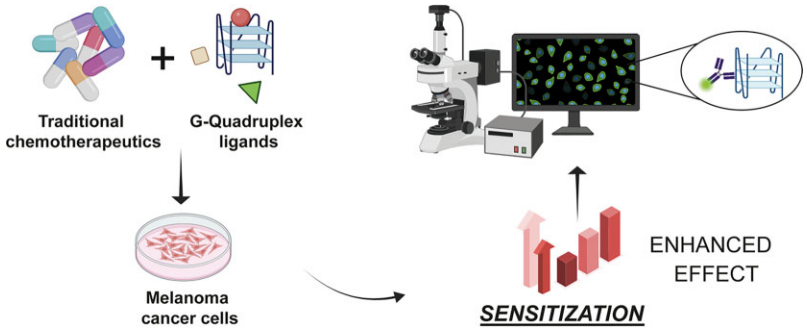

Introduction

Cancer ranks among the deadliest pathological diseases worldwide. Its heterogeneity, altered metabolism, epigenetic changes and several other molecular features make it an awfully intricate model that has conquered researchers' attention for decades and still raises questions for a comprehensive understanding of its molecular basis (1).

Currently, traditional chemotherapy remains a primary therapeutic option in the fight against cancer. This approach involves using drugs to target and inhibit biological processes that are crucial for the replication of fast-dividing tumor cells. In this regard, a plethora of chemotherapeutic agents have been devised over the years, differing from each other in their chemical nature and/or mechanism of action, as reviewed elsewhere (2).

Despite the significant success of conventional chemotherapeutics in clinical practice, which has substantially increased the overall survival rate of cancer patients, the adverse

Received: July 27, 2024. **Revised:** September 13, 2024. **Editorial Decision:** October 10, 2024. **Accepted:** October 17, 2024

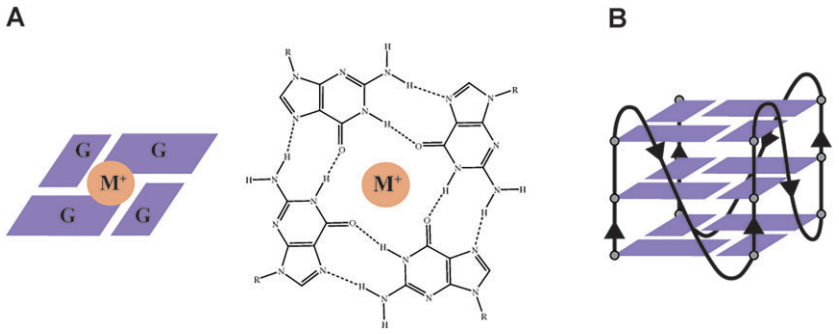

Figure 1. (**A**) The guanine tetrad, where M^+ is a monovalent cation. (**B**) An example of G4 structure.

effects of chemotherapy on patients' physical and psychological health can be severe.

In the last decades, significant research efforts have focused on exploring alternative anticancer strategies. Among these, a promising approach includes the targeting of noncanonical DNA secondary structures. Beyond the double-helical structure (B-DNA) described by Watson and Crick in 1953 (3), DNA can also adopt alternative conformations, such as hairpins, cruciforms, triple helices and G-quadruplexes (G4s) (4). These structures differ from the canonical double helix and may serve as highly specific and effective molecular targets. Among those mentioned above, G4s stand out as the most broadly studied alternative structures of DNA (5). They are stable four-stranded helical conformations that can arise from guanine-rich DNA sequences through the self-stacking of two or more guanine tetrads (Figure 1) (6). Intriguingly, it has been shown that sequences able to fold into G4s mainly exist at specific genomic loci (i.e. telomeres and gene promoters) (7,8), taking part in the regulation of fundamental biological processes such as telomere homeostasis and gene transcription (5,9,10).

Numerous studies have shown that G4 formation/stabilization can impair telomerase activity or reduce oncogene transcription efficiency (11,10). As a result, cancer research has been actively pushed toward the development of compounds able to induce G4 formation or stabilize endogenous G4 structures (12–15).

In this context, we systematically combined seven standard chemotherapeutic drugs each with a different mode of action, such as azacytidine, 5-fluorouracil (5-FU), methotrexate, cisplatin, doxorubicin, paclitaxel or vincristine, with three G4 binders, namely berberine, pyridostatin (PDS) and RHPS4, to enhance their antitumoral activity against melanoma cancer cells. Intriguingly, we found synergistic interactions between the vast majority of the anticancer drugs and G4 binders included in the study. Importantly, some of the most synergistic combinations also demonstrated selective toxicity toward melanoma cells over nontumorigenic human keratinocytes. Finally, we provided first evidence for the potential involvement of G4 structures in the outstanding synergism between some chemotherapeutics and G4 ligands.

Materials and methods

Materials

Dulbecco's modified Eagle's medium (DMEM), Dulbecco's phosphate buffered saline (PBS), fetal bovine serum (FBS), penicillin, streptomycin and cell culture plasticware were provided by Euroclone S.p.A. (Milan, Italy). L-Glutamine was purchased from Thermo Fisher Scientific (Waltham, MA, USA). Dimethyl sulfoxide (DMSO), 4% paraformaldehyde, Triton X-100 and bovine serum albumin (BSA) were supplied by HiMedia (Pennsylvania, USA).

The following antibodies were used for the immunofluorescence experiments: anti-DNA G4 structures, clone BG4 (Merck Millipore, Prague, Czech Republic, #MABE917); rabbit anti-FLAG antibody (Merck, St Louis, MO, USA, #F7425); donkey anti-rabbit IgG (H + L) highly cross-adsorbed secondary antibody (Alexa Fluor 488 Conjugate) (Thermo Fisher Scientific, Waltham, MA, USA, #A-21206).

The Hoechst 33258 solution, Mowiol 4-88, the Cell Proliferation Kit (MTT), azacytidine, cisplatin, doxorubicin, 5-FU, methotrexate, paclitaxel, vincristine, berberine and RHPS4 were purchased from Merck (St Louis, MO, USA). PDS was provided by Aurogene S.r.l. (Rome, Italy).

Cell culture

A375MM human melanoma cells were grown in DMEM supplemented with 10% FBS, 100 U/ml penicillin and 100 μg/ml streptomycin. Human epidermal keratinocytes (HaCaT cells) were purchased from CEINGE Biotecnologie Avanzate—Franco Salvatore Cell Culture Facility and grown in DMEM supplemented with 10% FBS, antibiotics and 2 mM L-glutamine. Both A375MM and HaCaT cells were subcultured at 90% confluence every 3 days and maintained at 37°C in a humidified atmosphere containing 5% CO_2.

The chemotherapeutics and the G4 ligands used in this study were dissolved in 100% DMSO to make stock solutions at 200 mM (for PDS), 80 mM (for azacytidine, berberine and RHPS4), 40 mM (for 5-FU, methotrexate and vincristine) or 20 mM (for doxorubicin and paclitaxel) concentration. As for cisplatin, a 5 mM stock solution in 0.9% NaCl was prepared. Each tested compound was diluted in cell culture medium to the required concentration, immediately prior to use.

Cell viability assay

The MTT assay was employed to detect cell viability (16). Briefly, A375MM cells (7000 cells/well) or HaCaT cells (20 000 cells/well) were seeded in 96-well plates and incubated at 37°C for 24 h. For the 48-h simultaneous treatments, the medium was then removed and cells were incubated with fresh medium containing increasing concentrations of chemotherapeutic and G4 ligand in simultaneous combination. As regards the sequential treatments, cells were exposed to increasing concentrations of chemotherapeutic (24 h) fol-

Table 1. Description of synergism, additivity or antagonism in drug combination studies performed with the Chou–Talalay method (19)

Range of CI	Description
<0.10	Very strong synergism
0.10–0.30	Strong synergism
0.30–0.70	Synergism
0.70–0.85	Moderate synergism
0.85–0.90	Slight synergism
0.90–1.10	Nearly additive
1.10–1.20	Slight antagonism
1.20–1.45	Moderate antagonism
1.45–3.30	Antagonism
3.30–10	Strong antagonism
>10	Very strong antagonism

lowed by increasing concentrations of G4 binder (further 24 h) or vice versa (17). The 24- and 48-h cytotoxicity profiles of each G4 ligand or chemotherapeutic alone, on A375MM cells, were also delineated (Supplementary Figures S1–S6). At the end of the treatments, 10 μl of MTT reagent was added to each well, at a final concentration of 0.5 mg/ml, and the plates were incubated at 37°C for 4 h. The resulting purple formazan crystals were dissolved by adding 100 μl of the solubilization solution to each well and the plates were then allowed to stand overnight in the incubator. Finally, the absorbance of the samples (at 570 nm) was measured on an ELx800 Absorbance Microplate Reader (BioTek Instruments, Inc., Winooski, VT, USA) and the percentage (%) of cell survival for each condition was calculated as follows:

$$\%\ \text{cell survival} = \frac{\text{Abs} - \text{Abs}_0}{\text{Abs}_{\text{Control}} - \text{Abs}_0} \times 100, \quad (1)$$

where Abs is the absorbance of the sample, Abs_0 is the absorbance of the background signal and $\text{Abs}_{\text{Control}}$ is the absorbance of the control sample (cells treated with the proper amount of vehicle). The concentration of compound able to reduce by 50% the cellular viability (IC_{50}) was calculated through a nonlinear regression analysis, using Prism 8.0.2 (GraphPad, San Diego, CA, USA).

Analysis of drug–drug interaction

The IC_{50} value of each drug, alone or in combination, was used to determine the corresponding combination index (CI), according to the Chou–Talalay method (18). Particularly, for a two-drug combination, the model can be written as follows:

$$\text{CI} = \left(\frac{D_1}{D_{x1}}\right) + \left(\frac{D_2}{D_{x2}}\right), \quad (2)$$

where D_1 is the IC_{50} of Drug 1 in the combination, D_{x1} is the IC_{50} of Drug 1 alone, D_2 is the IC_{50} of Drug 2 in the combination and D_{x2} is the IC_{50} of Drug 2 alone.

Overall, CI values <0.90 denoted synergism, CI values >1.10 indicated antagonism and CI values in the range 0.90–1.10 implied an additive effect (see Table 1).

The dose-reduction index (DRI) (19) for each drug in a synergistic combination was also calculated to assess the magnitude of dose reduction allowed, compared to each drug alone:

$$\text{DRI} = \frac{D_x}{D}, \quad (3)$$

which is a simple inversion of Equation (2).

DRI values below, above and equal to 1 indicated not favorable dose reduction, favorable dose reduction and no dose reduction for each drug in the combination, respectively.

Selectivity index calculation

Whenever possible, the selectivity index (SI) of the drugs involved in the most promising synergistic combinations (within the tested range of drug concentrations) was calculated, employing the following formula:

$$\text{SI} = \frac{IC_{50}\text{ against HaCaT cells}}{IC_{50}\text{ against melanoma cells}}, \quad (4)$$

SI values below or above 1 indicated toxicity or desirable selectivity against melanoma cancer cells, respectively. An SI > 2 denoted high selectivity (20,21).

Immunofluorescence studies

A375MM cells were seeded on sterile coverslips, in a 24-well plate, at a density of 90 000 cells per well, and incubated overnight. Then, for the 48-h simultaneous treatments, cells received either vehicle (0.1% DMSO) or a sublethal concentration of each tested drug (alone or in simultaneous combination), for 48 h. As for the sequential treatments, cells were exposed to vehicle (0.1% DMSO) or to a sublethal concentration of each investigated drug alone (24 h) or in consecutive combination (24 h → 24 h). At the end of the treatments, A375MM cells were fixed in 4% paraformaldehyde (v/v), at room temperature (RT), for 10 min, and permeabilized in 0.1% Triton X-100 (v/v) in PBS, at RT for 10 min. Nonspecific binding sites were blocked with 5% BSA (w/v) in PBS, at RT for 30 min. Cells were then incubated with the BG4 antibody (1:100), at RT for 1 h, rinsed three times with PBS and incubated with the rabbit anti-FLAG antibody (1:2500), at RT for 1 h. After three more rinsing steps with PBS, cells were incubated with the anti-rabbit Alexa Fluor 488 Conjugate secondary antibody (1:500), at RT for 1 h. Nuclei were counterstained with the Hoechst 33258 solution (1:3000, 10 min). Finally, coverslips were rinsed once with distilled water and mounted on microscope slides with Mowiol 4-88.

As for the image acquisition, *z*-stacks of six planes were recorded by means of a confocal microscope (Zeiss LSM 980, Plan-Apochromat 63×/1.4 NA oil objective). For the image analysis, a maximum intensity projection of each *z*-stack was generated. From there, the nuclear foci were segmented, and their number was quantified by using the Image Analysis package of ZEISS ZEN Blue 3.1 software. The statistical details of all experiments are reported in the figure legends.

Results and discussion

The combination of standard chemotherapeutics with G4 binders shows synergistic anticancer effects

In order to investigate the effects of combining G4 ligands with chemotherapeutic agents, *in vitro* MTT assays (16) were performed. Particularly, A375MM melanoma cells were treated with commonly used antineoplastic drugs (azacytidine, 5-FU, methotrexate, cisplatin, doxorubicin, paclitaxel or vincristine) in simultaneous combination with well-characterized G4 binders (berberine, PDS or RHPS4; Supplementary Figure S7) (22–24), for 48 h. Afterward, the Chou–Talalay method was used to calculate the CI values

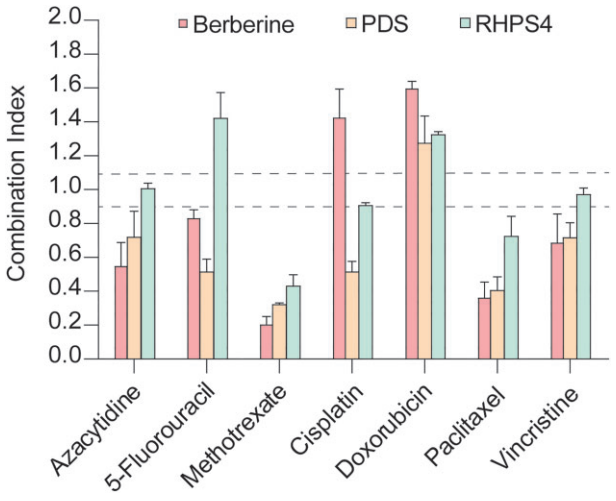

Figure 2. Graphic visualization of the CI values obtained from the 48-h simultaneous treatments on A375MM melanoma cells. Histograms show the mean ± standard deviation (SD) of two independent experiments. Calculated CI and IC_{50} values are reported in Supplementary Tables S1 and S2, whereas MTT data are collected in Supplementary Figures S8–S13.

from our MTT assays, providing a quantitative assessment of the interactions between the combined agents (see the 'Materials and methods' section) (25). As shown in Table 1, specific ranges of CI values indicated the extent of synergistic, additive and antagonistic effects for the drug combinations.

Interestingly, the investigated combinations produced quite different results. As highlighted in Figure 2 and Supplementary Table S1, only five combinations resulted in antagonism (CI > 1.10). Specifically, antagonistic effects were observed when doxorubicin was associated with berberine, PDS or RHPS4. This might be due to the G4-interacting properties of doxorubicin (26), which could thus compete with the G4 ligands for binding to G4 structures. Antagonism was also found between 5-FU and RHPS4, as well as when combining cisplatin with berberine.

On the other hand, three combinations resulted in a nearly additive effect (0.90 < CI < 1.10), meaning that the effect of the drug association was approximately equal to the sum of the effects of the drugs when given alone. All these combinations involved the use of RHPS4 (paired with azacytidine, cisplatin or vincristine), yielding CI values of 1.02 ± 0.03, 0.92 ± 0.02 and 0.98 ± 0.04, respectively.

Of note, the vast majority of the anticancer drugs included in the study showed a synergistic interaction with the G4 binders (CI < 0.90). Interestingly, PDS was the only G4 ligand that significantly synergized with cisplatin, giving a CI of 0.52 ± 0.06. We cannot exclude that this effect is due to the formation of a complex between the amine groups of PDS and the platinum atom of cisplatin, resulting in stronger G4-binding capability. Such hypothesis might be supported by a recent study from Ma *et al.*, who synthesized platinum complexes combining cisplatin and a PDS derivative. These complexes demonstrated enhanced specificity for G4 domains (27). Furthermore, among the associations with 5-FU, PDS produced the strongest synergistic effect (CI of 0.53 ± 0.08).

Nevertheless, the most impressive results were obtained with the treatments involving paclitaxel and methotrexate as chemotherapeutics. Indeed, the cytotoxic effects of paclitaxel against A375MM cells were strongly enhanced by the alkaloid berberine (CI = 0.34 ± 0.03), suggesting an interesting and powerful cooperation between the two agents. Moreover, in line with recent findings on other *in vitro* (and *in vivo*) models (28), synergism between paclitaxel and the bisquinoline PDS was also confirmed in our experiments (CI = 0.41 ± 0.08). A synergistic interaction, albeit moderate, was also obtained when paclitaxel was combined with the acridine RHPS4, as evidenced by the corresponding CI value of 0.73 ± 0.12.

Similarly, the cytotoxicity of methotrexate toward melanoma cells was greatly enhanced by its association with both berberine and PDS (CI values of 0.22 ± 0.04 and 0.33 ± 0.01, respectively). Methotrexate and RHPS4 also acted synergistically, even if to a lesser extent (CI = 0.44 ± 0.07).

Furthermore, in order to estimate to which extent the dose of the drugs in combination could be reduced as a result of synergism, DRI values were calculated for all synergistic combinations. DRI values below, above and equal to 1 indicated unfavorable dose reduction, favorable dose reduction and no dose reduction for each drug in combination, respectively. Importantly, under the experimental conditions employed, all DRI values were above 1 for both the chemotherapeutics and the G4 ligands (Table 2). Particularly, the DRI values of methotrexate combined with each of the three G4 ligands were exceptionally high, allowing to decrease its doses from the micromolar to the low nanomolar range.

In summary, the simultaneous association of chemotherapeutics and G4 ligands for 48 h produced antagonism and additivity in some cases. However, synergism was detected for most of the combinations. Noteworthy, among all the simultaneous treatments, the combination of methotrexate with berberine stood out, showing the lowest CI value and the highest DRI value for the chemotherapeutic agent.

The extent of synergism between chemotherapeutics and G4 binders depends on sequence and timing of drug administration

The promising results arising from most simultaneous associations between chemotherapeutics and G4 ligands led us to explore whether varying the treatment schedule could affect the type and/or extent of the drug–drug interaction (17). Therefore, we performed sequential treatments where the two agents were administered to the cells one after the other (24 h → 24 h), keeping the overall treatment duration of 48 h. In detail, melanoma cells were first treated with the G4 binder (for 24 h), followed by the chemotherapeutic agent (for further 24 h), using the same ranges of drug concentrations as for the simultaneous treatments. The opposite approach, with cells pretreated with the chemotherapeutic (for 24 h) and then exposed to the G4 ligand (for further 24 h), was explored as well.

As for the 'G4 ligand → chemotherapeutic' treatments (Supplementary Figures S14–S18), when A375MM cells were exposed to berberine or RHPS4 followed by almost any of the investigated chemotherapeutics, the percentage of cell survival never fell below 50–60%, even at high drug concentrations. This high survival rate hampered the accurate calculation of the IC_{50} values for the combined drugs, making it impossible to calculate the CI values. However, the sequen-

Table 2. DRI values obtained from the 48-h simultaneous treatments on A375MM melanoma cells

Chemotherapeutic	DRI[a] for the combination with		
	Berberine	PDS	RHPS4
Azacytidine	2.70 ± 0.67	2.92 ± 0.59	-
	5.74 ± 1.47	2.72 ± 0.62	-
Cisplatin	-	5.12 ± 1.09	-
	-	3.10 ± 0.17	-
Doxorubicin	-	-	-
	-	-	-
5-FU	1.78 ± 0.11	4.28 ± 0.86	-
	3.59 ± 0.15	3.47 ± 0.36	-
Methotrexate	8840.00 ± 2885.00	3232.63 ± 297.56	8742.86 ± 1373.81
	4.74 ± 0.96	3.04 ± 0.08	2.29 ± 0.36
Paclitaxel	4.18 ± 0.21	4.21 ± 0.52	3.25 ± 0.22
	9.75 ± 1.89	5.98 ± 1.63	2.41 ± 0.54
Vincristine	1.78 ± 0.31	1.76 ± 0.16	-
	9.26 ± 5.07	6.61 ± 1.61	-

[a]DRI values were obtained using Equation (3) (see the 'Materials and methods' section), only for the combinations showing synergistic effects. Values are reported as mean ± SD of two independent experiments.
For each row, the value on the top is for the chemotherapeutic and the one at the bottom is for the G4 ligand.

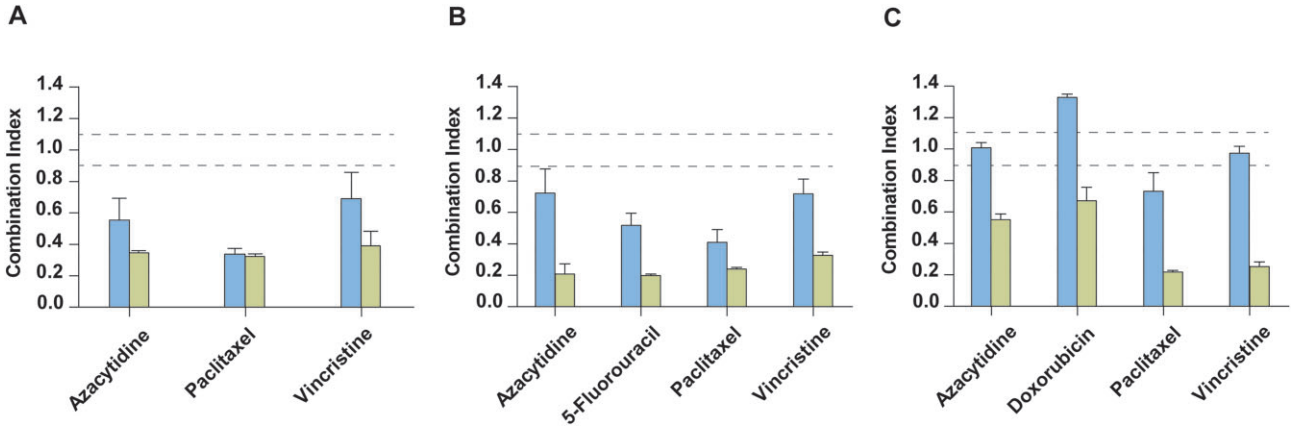

Figure 3. Graphic comparison of the CI values obtained from the simultaneous (bar on the left) and 'chemotherapeutic → G4 ligand' sequential (bar on the right) treatments for the associations with (**A**) berberine, (**B**) PDS and (**C**) RHPS4. Histograms show the mean ± SD of two independent experiments. Calculated CI and IC_{50} values for the 'chemotherapeutic → G4 ligand' sequential treatments are reported in Supplementary Tables S6 and S7.

tial treatment berberine → azacytidine still showed synergism (CI = 0.80 ± 0.01) (Supplementary Tables S3 and S4), although weaker than that resulting from the 48-h simultaneous schedule (CI = 0.56 ± 0.14) and associated with lower DRI values (Supplementary Table S5), while the treatment berberine → cisplatin still resulted in an antagonistic effect (CI = 1.28 ± 0.03). Surprisingly, sequential treatments with PDS followed by azacytidine, 5-FU or vincristine (24 h → 24 h) generally enhanced the synergistic interaction between the G4 binder and the chemotherapeutic agent, compared to the corresponding simultaneous combinations, with the CI values dropping from 0.73 ± 0.16, 0.53 ± 0.08 and 0.73 ± 0.09 (simultaneous schedule) to 0.21 ± 0.07, 0.48 ± 0.03 and 0.41 ± 0.01 (sequential schedule), respectively.

Nevertheless, the most remarkable results were observed when A375MM melanoma cells were pretreated with the chemotherapeutic and then exposed to the G4 binder ('chemotherapeutic → G4 ligand' treatments; Supplementary Figures S19–S24). Indeed, as shown in Figure 3, many of these sequential treatments proved to extraordinarily boost the drug–drug synergism compared to the simultaneous treatments, resulting in much lower CI values and generally higher DRI values (Supplementary Tables S6–S8). Notably, treatments with azacytidine, doxorubicin or vincristine followed by RHPS4 resulted in the actual onset of synergism, compared to the simultaneous schedule, with CI values decreasing from 1.02 ± 0.03, 1.34 ± 0.02 and 0.98 ± 0.04 (simultaneous schedule) to 0.56 ± 0.04, 0.68 ± 0.08 and 0.28 ± 0.03 (sequential schedule), respectively.

Overall, the nature and extent of the interaction between the investigated chemotherapeutics and G4 ligands proved to be strictly dependent on both the treatment schedule (simultaneous or sequential) and the drug sequence ('G4 ligand → chemotherapeutic' or 'chemotherapeutic → G4 ligand') employed.

Specific associations of chemotherapeutics with G4 binders are tumor-selective

Based on the MTT results, all the simultaneous/sequential drug combinations that showed CI values ranging from 0.10

Table 3. Simultaneous and sequential combinations selected for further studies

Selected combination	Treatment schedule	CI ± SD
Vincristine → RHPS4	Sequential	0.28 ± 0.03
5-FU → PDS	Sequential	0.20 ± 0.01
Paclitaxel → PDS	Sequential	0.24 ± 0.01
Paclitaxel → RHPS4	Sequential	0.23 ± 0.01
Methotrexate + berberine	Simultaneous	0.22 ± 0.04
Azacytidine → PDS	Sequential	0.22 ± 0.06
PDS → azacytidine	Sequential	0.21 ± 0.07

to 0.30 (i.e. strong synergism) were selected as the most promising ones to be further investigated (Table 3).

Particularly, to predict the therapeutic potential of the selected associations, their toxicity toward nontumorigenic human keratinocytes (HaCaT) (29) was also tested, using the same treatment schedules and ranges of drug concentrations exploited on A375MM cancer cells. Whenever possible, the SI for each combined agent was calculated by determining the ratio of the drug toxicity (IC_{50}) against nontumorigenic HaCaT cells to that against A375MM melanoma cells (see Equation (4) in the 'Materials and methods' section). SI values >1.0 favorably indicated tumor selectivity, with SI values >2.0 implying high selectivity (20,21).

As shown in Figure 4A, the sequential treatment vincristine → RHPS4 proved to be generally more toxic to HaCaT cells than A375MM cancer cells, resulting in unfavorable SI values of 0.92 ± 0.07 for the chemotherapeutic and 0.41 ± 0.26 for the G4 binder. Likewise, the sequential treatment 5-FU → PDS (Figure 4B) showed comparable cytotoxicity profiles on HaCaT and A375MM cells, with the corresponding SI values for both the chemotherapeutic and the G4 ligand falling below 1.

In contrast, the sequential treatments paclitaxel → PDS and paclitaxel → RHPS4 yielded SI values exceeding 2 (Figure 4C and D), indicating a highly selective toxicity (>2-fold) toward melanoma cells over nontumorigenic human keratinocytes, under the experimental conditions employed.

Nonetheless, the highest degree of cancer selectivity was achieved with the combinations methotrexate + berberine, azacytidine → PDS and PDS → azacytidine, as shown in Figure 4E–G. Indeed, in these cases, the IC_{50} values of the combined drugs on HaCaT cells could not be determined, since the percentage of cellular viability after the treatments remained above 50%.

Overall, our results revealed good to excellent tumor selectivity for five out of seven combinations, highlighting their promising therapeutic potential.

Potential implication of DNA G4 structures in the synergism

Having in our hands five highly synergistic and tumor-selective drug combinations, we sought to investigate the potential involvement of DNA G4 structures in the synergism. For this purpose, A375MM cells were treated with either vehicle (0.1% DMSO) or sublethal concentrations of the tested drugs (alone or in combination), fixed with 4% paraformaldehyde, and then processed for immunofluorescence microscopy using the BG4 antibody, which selectively recognizes G4 structures (30).

Our results indicated that the nuclear G4 structures did not significantly change after the exposure to the sequential associations paclitaxel → PDS, PDS → azacytidine and azacytidine → PDS (Supplementary Figures S25 and S26). These findings imply that G4 structures may not be involved in the synergistic interaction between paclitaxel (or azacytidine) and the G4 binder PDS, at least in melanoma cells.

Conversely, A375MM cells treated with paclitaxel followed by RHPS4 (paclitaxel → RHPS4) exhibited a significant increase in nuclear G4 foci (Figure 5).

Similarly, Figure 6 reveals that treating A375MM cells with methotrexate or berberine alone did not significantly change the amount of nuclear G4 structures. However, when cells were exposed to both agents at the same time, the number of G4 structures increased by ∼30%.

In summary, these results suggest that the synergistic effects of specific combinations of chemotherapeutics and G4 ligands may be correlated to the formation of nuclear G4 structures that might play a crucial role for the efficacy of such treatments.

Conclusions

The general toxicity of traditional chemotherapy poses a critical hurdle in cancer management, adversely impacting the patients' quality of life. Herein, with the aim of reducing the required doses and, hopefully, the toxicity of chemotherapeutics, a systematic investigation was undertaken by combining standard antineoplastic drugs (azacytidine, 5-FU, methotrexate, cisplatin, doxorubicin, paclitaxel or vincristine) with G4 binders (berberine, PDS and RHPS4) on melanoma cancer cells.

Intriguingly, we found synergistic interactions between most of the anticancer drugs and G4 binders included in the study. Interestingly, our data also indicated that the extent of synergism between chemotherapeutics and G4 ligands varied significantly according to both the treatment schedule (simultaneous or sequential) and the sequence of drug administration ('G4 ligand → chemotherapeutic' or 'chemotherapeutic → G4 ligand').

Particularly, the simultaneous association (for 48 h) of the antimetabolite methotrexate with berberine, PDS or RHPS4 provided the strongest synergistic effects among all the simultaneous treatments and should be preferred over their sequential combination (24 h → 24 h) to achieve marked synergism. Conversely, we found that chemotherapeutics such as azacytidine, paclitaxel or vincristine should be given 24 h before the G4 binder to trigger strong synergism.

Importantly, five out of the seven most synergistic combinations also demonstrated selective toxicity toward melanoma cells over nontumorigenic human keratinocytes, proving a promising therapeutic potential.

Furthermore, immunofluorescence studies provided evidence for the potential implication of G4 structures in the biological mechanisms underlying the outstanding synergistic interaction between methotrexate and berberine, as well as paclitaxel and RHPS4, against melanoma cancer cells.

Overall, our systematic investigation supports the potential synergism between G4-interacting molecules and standard antineoplastic drugs (17,31). Such association might enhance the efficacy of traditional chemotherapeutics, potentially allowing for reduced doses in treatments. Additional studies are currently underway in our laboratory to unveil the molecular basis of this synergistic interaction and to validate these findings *in vivo*.

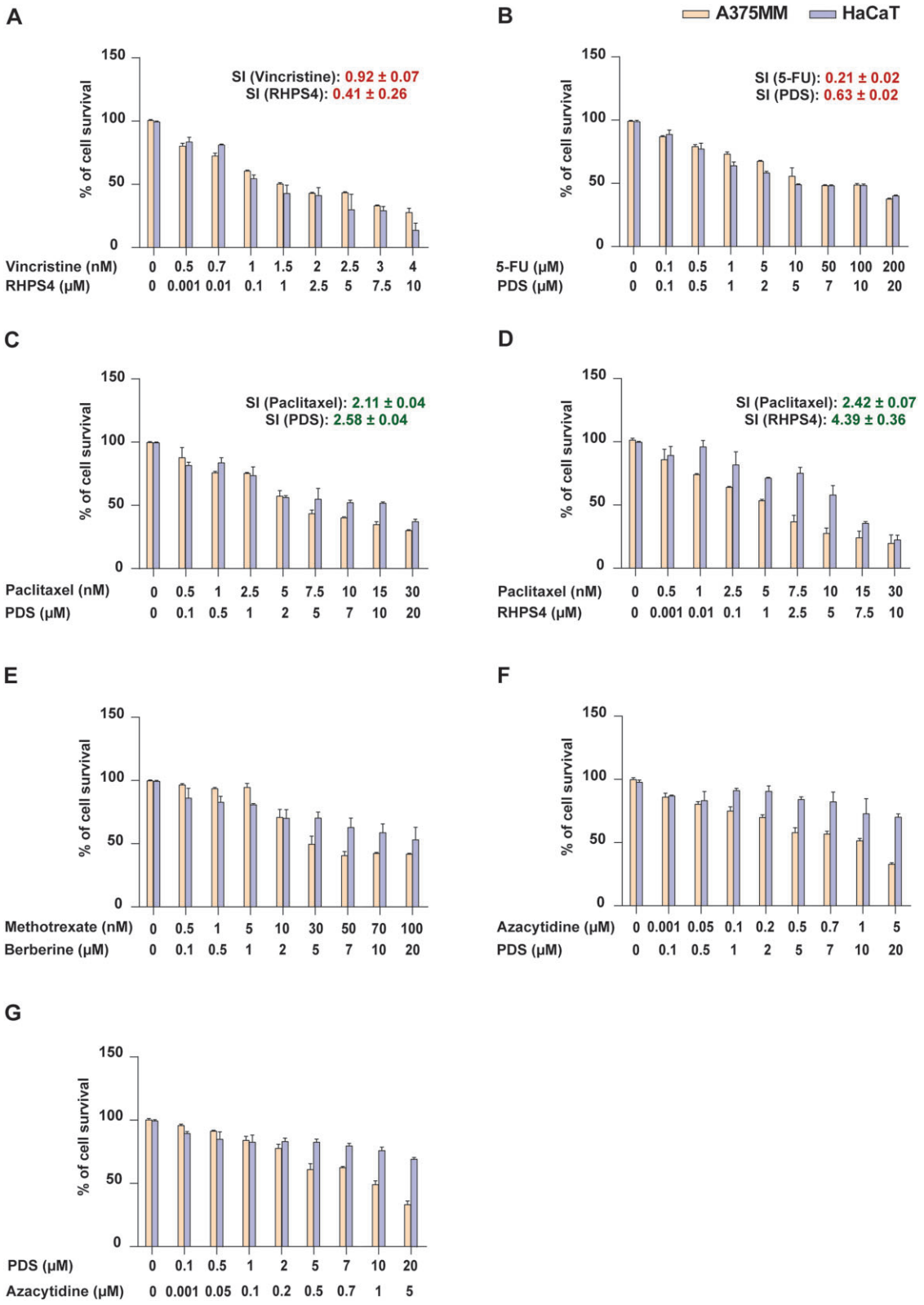

Figure 4. MTT cytotoxicity profiles of the seven selected combinations on A375MM melanoma cells and nontumorigenic HaCaT cells, obtained under the same experimental conditions. The IC_{50} values on A375MM melanoma cells and nontumorigenic HaCaT cells are reported in Supplementary Table S9.

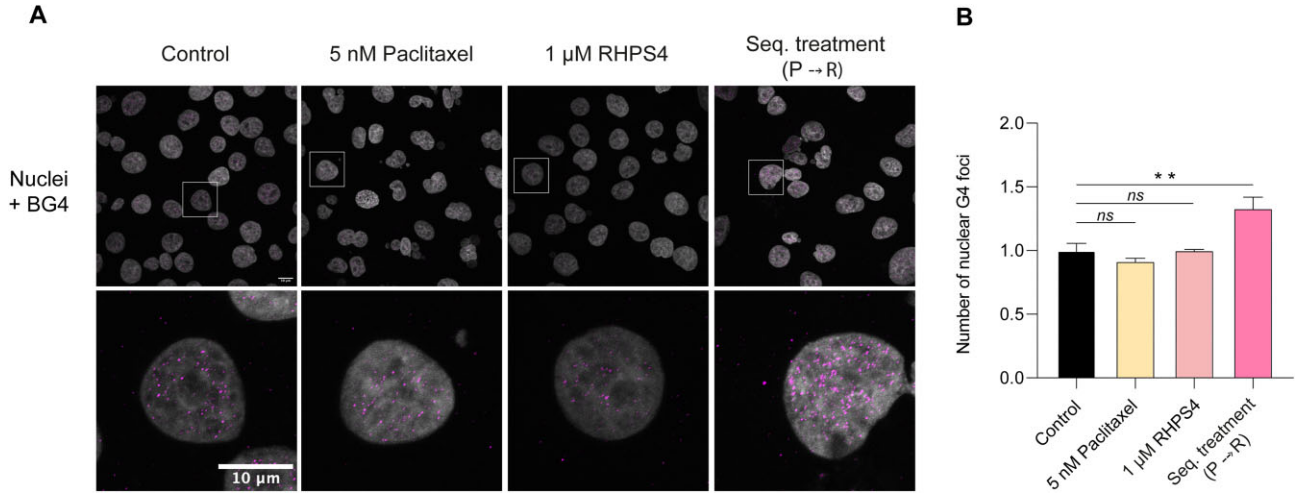

Figure 5. (**A**) Representative fields showing G4 foci formation detected by immunofluorescence in A375MM cells treated for 24 h with 0.1% DMSO (control), 5 nM paclitaxel or 1 μM RHPS4. As for the sequential treatment (P → R), A375MM cells were exposed to 5 nM paclitaxel (for 24 h) followed by 1 μM RHPS4 (for another 24 h). Scale bar: 10 μm. Upper panels: The merged channels of BG4-stained G4 structures (magenta) and Hoechst-counterstained nuclei (gray) are reported. Lower panels: Enlargements from the pictures in the upper panels. (**B**) Quantitative analysis of the nuclear G4 foci. An average of 60 cells were screened for each condition and the results are expressed as fold change over the negative control (DMSO-treated cells). Histograms show the mean ± SD of two independent experiments. The statistical significance was calculated using a one-way ANOVA test on GraphPad Prism 8.0.2 (**$P < 0.01$).

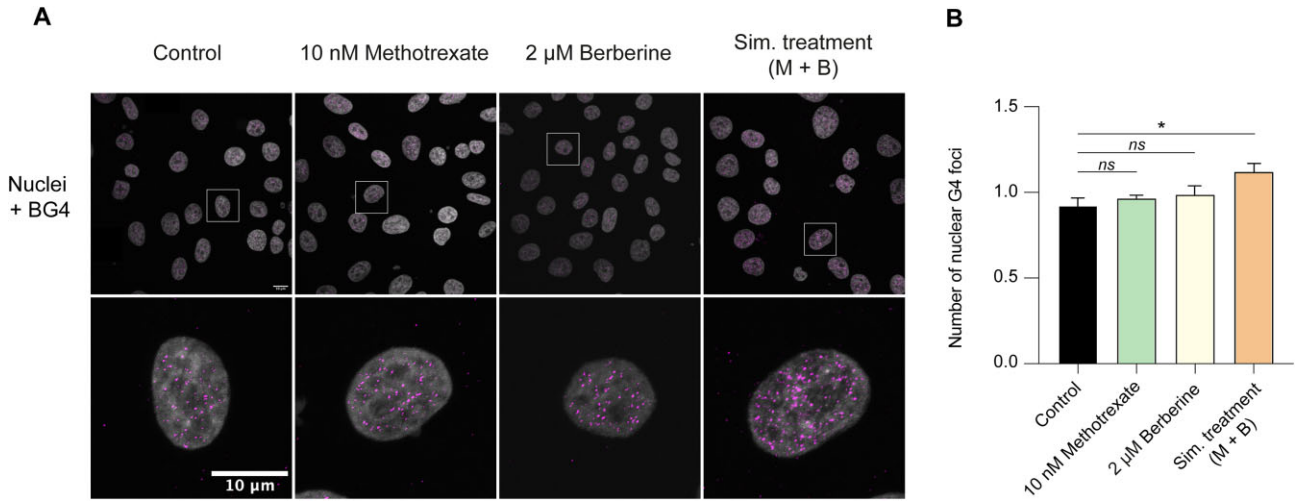

Figure 6. (**A**) Representative fields showing G4 foci formation detected by immunofluorescence in A375MM cells treated for 48 h with 0.1% DMSO (control), 10 nM methotrexate, 2 μM berberine or 10 nM methotrexate + 2 μM berberine. Scale bar: 10 μm. Upper panels: The merged channels of BG4-stained G4 structures (magenta) and Hoechst-counterstained nuclei (gray) are reported. Lower panels: Enlargements from the pictures in the upper panels. (**B**) Quantitative analysis of the nuclear G4 foci. An average of 60 cells were screened for each condition and the results are expressed as fold change over the negative control (DMSO-treated cells). Histograms show the mean ± SD of two independent experiments. The statistical significance was calculated using a one-way ANOVA test on GraphPad Prism 8.0.2 (*$P < 0.05$).

Data availability

The data underlying this article are available in the article and in its online supplementary material.

Supplementary data

Supplementary Data are available at NAR Cancer Online.

Acknowledgements

Microscopy experiments were done at the CEINGE Advanced Light Microscopy Facility.

Funding

Italian Association for Cancer Research (AIRC) [IG #26313 to A.R.].

Conflict of interest statement

None declared.

References

1. Harris,T.J.R. and McCormick,F. (2010) The molecular pathology of cancer. *Nat. Rev. Clin. Oncol.*, 7, 251–265.

2. Anand,U., Dey,A., Chandel,A.K.S., Sanyal,R., Mishra,A., Pandey,D.K., De Falco,V., Upadhyay,A., Kandimalla,R., Chaudhary,A., *et al.* (2022) Cancer chemotherapy and beyond: current status, drug candidates, associated risks and progress in targeted therapeutics. *Genes Dis.*, **10**, 1367–1401.
3. Watson,J.D. and Crick,F.H.C. (1953) Molecular structure of nucleic acids: a structure for deoxyribose nucleic acid. *Nature*, **171**, 737–738.
4. Choi,J. and Majima,T. (2011) Conformational changes of non-B DNA. *Chem. Soc. Rev.*, **40**, 5893.
5. Spiegel,J., Adhikari,S. and Balasubramanian,S. (2020) The structure and function of DNA G-quadruplexes. *Trends Chem.*, **2**, 123–136.
6. Huppert,J.L. (2010) Structure, location and interactions of G-quadruplexes. *FEBS J.*, **277**, 3452–3458.
7. Marsico,G., Chambers,V.S., Sahakyan,A.B., McCauley,P., Boutell,J.M., Antonio,M.D. and Balasubramanian,S. (2019) Whole genome experimental maps of DNA G-quadruplexes in multiple species. *Nucleic Acids Res.*, **47**, 3862–3874.
8. Romano,F., Di Porzio,A., Iaccarino,N., Riccardi,G., Di Lorenzo,R., Laneri,S., Pagano,B., Amato,J. and Randazzo,A. (2023) G-quadruplexes in cancer-related gene promoters: from identification to therapeutic targeting. *Expert Opin. Ther. Pat.*, **33**, 745–773.
9. Rhodes,D. and Lipps,H.J. (2015) G-quadruplexes and their regulatory roles in biology. *Nucleic Acids Res.*, **43**, 8627–8637.
10. Kim,N. (2019) The interplay between G-quadruplex and transcription. *Curr. Med. Chem.*, **26**, 2898–2917.
11. Bryan,T.M. (2020) G-quadruplexes at telomeres: friend or foe? *Molecules*, **25**, 3686.
12. Carvalho,J., Mergny,J.-L., Salgado,G.F., Queiroz,J.A. and Cruz,C. (2020) G-quadruplex, friend or foe: the role of the G-quartet in anticancer strategies. *Trends Mol. Med.*, **26**, 848–861.
13. Di Porzio,A., Galli,U., Amato,J., Zizza,P., Iachettini,S., Iaccarino,N., Marzano,S., Santoro,F., Brancaccio,D., Carotenuto,A., *et al.* (2021) Synthesis and characterization of bis-triazolyl-pyridine derivatives as noncanonical DNA-interacting compounds. *Int. J. Mol. Sci.*, **22**, 11959.
14. Sun,Z.-Y., Wang,X.-N., Cheng,S.-Q., Su,X.-X. and Ou,T.-M. (2019) Developing novel G-quadruplex ligands: from interaction with nucleic acids to interfering with nucleic acid–protein interaction. *Molecules*, **24**, 396.
15. Figueiredo,J., Mergny,J.-L. and Cruz,C. (2024) G-quadruplex ligands in cancer therapy: progress, challenges, and clinical perspectives. *Life Sci.*, **340**, 122481.
16. Mosmann,T. (1983) Rapid colorimetric assay for cellular growth and survival: application to proliferation and cytotoxicity assays. *J. Immunol. Methods*, **65**, 55–63.
17. Leonetti,C., Scarsella,M., Riggio,G., Rizzo,A., Salvati,E., D'Incalci,M., Staszewsky,L., Frapolli,R., Stevens,M.F., Stoppacciaro,A., *et al.* (2008) G-quadruplex ligand RHPS4 potentiates the antitumor activity of camptothecins in preclinical models of solid tumors. *Clin. Cancer Res.*, **14**, 7284–7291.
18. Chou,T.-C. (2010) Drug combination studies and their synergy quantification using the Chou–Talalay method. *Cancer Res.*, **70**, 440–446.
19. Chou,T.C. (2006) Theoretical basis, experimental design, and computerized simulation of synergism and antagonism in drug combination studies. *Pharmacol. Rev.*, **58**, 621–681.
20. Machana,S., Weerapreeyakul,N., Barusrux,S., Nonpunya,A., Sripanidkulchai,B. and Thitimetharoch,T. (2011) Cytotoxic and apoptotic effects of six herbal plants against the human hepatocarcinoma (HepG2) cell line. *Chin. Med.*, **6**, 39.
21. Prayong,P., Barusrux,S. and Weerapreeyakul,N. (2008) Cytotoxic activity screening of some indigenous Thai plants. *Fitoterapia*, **79**, 598–601.
22. Dickerhoff,J., Brundridge,N., McLuckey,S.A. and Yang,D. (2021) Berberine molecular recognition of the parallel MYC G-quadruplex in solution. *J. Med. Chem.*, **64**, 16205–16212.
23. Rodriguez,R., Müller,S., Yeoman,J.A., Trentesaux,C., Riou,J.-F. and Balasubramanian,S. (2008) A novel small molecule that alters shelterin integrity and triggers a DNA-damage response at telomeres. *J. Am. Chem. Soc.*, **130**, 15758–15759.
24. Gavathiotis,E., Heald,R.A., Stevens,M.F.G. and Searle,M.S. (2003) Drug recognition and stabilisation of the parallel-stranded DNA quadruplex d(TTAGGGT)$_4$ containing the human telomeric repeat. *J. Mol. Biol.*, **334**, 25–36.
25. Chou,T.-C. and Talalay,P. (1984) Quantitative analysis of dose–effect relationships: the combined effects of multiple drugs or enzyme inhibitors. *Adv. Enzyme Regul.*, **22**, 27–55.
26. Scaglioni,L., Mondelli,R., Artali,R., Sirtori,F.R. and Mazzini,S. (2016) Nemorubicin and doxorubicin bind the G-quadruplex sequences of the human telomeres and of the c-MYC promoter element Pu22. *Biochim. Biophys. Acta Gen. Subj.*, **1860**, 1129–1138.
27. Ma,T.Z., Liu,L.Y., Zeng,Y.L., Ding,K., Zhang,H., Liu,W., Cao,Q., Xia,W., Xiong,X., Wu,C., *et al.* (2024) G-quadruplex-guided cisplatin triggers multiple pathways in targeted chemotherapy and immunotherapy. *Chem. Sci.*, **15**, 9756–9774.
28. Groelly,F.J., Porru,M., Zimmer,J., Benainous,H., De Visser,Y., Kosova,A.A., Di Vito,S., Serra,V., Ryan,A., Leonetti,C., *et al.* (2022) Anti-tumoural activity of the G-quadruplex ligand pyridostatin against BRCA1/2-deficient tumours. *EMBO Mol. Med.*, **14**, e14501.
29. Boukamp,P., Petrussevska,R.T., Breitkreutz,D., Hornung,J., Markham,A. and Fusenig,N.E. (1988) Normal keratinization in a spontaneously immortalized aneuploid human keratinocyte cell line. *J. Cell Biol.*, **106**, 761–771.
30. Biffi,G., Tannahill,D., McCafferty,J. and Balasubramanian,S. (2013) Quantitative visualization of DNA G-quadruplex structures in human cells. *Nat. Chem.*, **5**, 182–186.
31. Gunaratnam,M., Green,C., Moreira,J.B., Moorhouse,A.D., Kelland,L.R., Moses,J.E. and Neidle,S. (2009) G-quadruplex compounds and *cis*-platin act synergistically to inhibit cancer cell growth *in vitro* and *in vivo*. *Biochem. Pharmacol.*, **78**, 115–122.

Received: July 27, 2024. **Revised:** September 13, 2024. **Editorial Decision:** October 10, 2024. **Accepted:** October 17, 2024